

Microwave background anisotropies and nonlinear structures I. Improved theoretical models

A.N. Lasenby^{*}, C.J.L. Doran, M.P. Hobson, Y. Dabrowski and A.D. Challinor

Mullard Radio Astronomy Observatory, Cavendish Laboratory, Madingley Road, Cambridge CB3 0HE, UK

Accepted ????. Received ???; in original form 1 February 2008

ABSTRACT

A new method is proposed for modelling spherically symmetric inhomogeneities in the Universe. The inhomogeneities have finite size and are compensated, so they do not exert any measurable gravitational force beyond their boundary. The region exterior to the perturbation is represented by a Friedmann-Robertson-Walker (FRW) Universe, which we use to study the anisotropy in the cosmic microwave background (CMB) induced by the cluster. All calculations are performed in a single, global coordinate system, with nonlinear gravitational effects fully incorporated. An advantage of the gauge choices employed here is that the resultant equations are essentially Newtonian in form. Examination of the problem of specifying initial data shows that the new model presented here has many advantages over ‘Swiss cheese’ and other models. Numerical implementation of the equations derived here is described in a subsequent paper.

Key words: Gravitation – cosmology: theory – cosmology : gravitational lensing – cosmic microwave background – galaxies: clustering

1 INTRODUCTION

Many attempts have been made to model secondary anisotropies in the cosmic microwave background (CMB) due to galaxy clusters. The most widely employed approach is to use a linearised set of equations to incorporate gravitational effects (Landau & Lifshitz 1975; Martínez-González, Sanz & Silk 1990; Martínez-González & Sanz 1990; Chodorowski 1991; Pyne & Birkinshaw 1996). This has the advantage that one can deal with quite general matter perturbations, avoiding the restrictions of spherical symmetry imposed by most other methods. Doubts always remain, however, over the accuracy of calculations performed in the linearised theory, and it is only through comparison with models incorporating full, nonlinear effects that any errors can be reliably computed.

The earliest attempts to calculate anisotropies in the full, nonlinear theory employed ‘Swiss cheese’ models (Rees & Sciama 1968; Dyer 1976; Kaiser 1982; Nottale 1982a; Nottale 1982b; Nottale 1983; Nottale 1984). In these models a collapsing FRW Universe is surrounded by a compensating vacuum region, which then matches onto an exterior expanding FRW Universe. The compensating region ensures that the perturbation has no net gravitational effect on the exterior Universe. These models have two key advantages: analytic calculations can be performed in the fully nonlinear

regime; and all observations can be modelled in the exterior region, providing clear, unambiguous predictions of the effect of the cluster. The main disadvantage of such models is that the matter distribution is unrealistic, and appears to overestimate the effect of the cluster (Quilis, Ibáñez & Sáez 1995).

More realistic models can be constructed by working with an arbitrary density profile while restricting to spherical symmetry and ignoring pressure (Panek 1992; Arnau et al. 1993; Sáez, Arnau & Fullana 1993; Arnau, Fullana & Sáez 1994; Fullana, Sáez & Arnau 1994; Quilis & Sáez 1998). Spherically symmetric models with vanishing pressure have implicit analytic solutions in General Relativity, one simple form of which is provided by the Tolman-Bondi solution (Tolman 1934; Bondi 1947). Models based on this solution provide a more reliable method for computing anisotropies due to clusters or voids, and it is a hybrid of this scheme that we discuss here. Previous work with Tolman-Bondi models has considered density and velocity perturbations, but compensating effects are not usually included. (One exception to this is the ‘type I’ class of models considered by Panek (1992), but these are only compensated at infinity.) The fact that observers comoving with the fluid are not in a region modelled by a homogeneous FRW cosmology makes it harder to discuss perturbations, since these observers see a dipole anisotropy in the CMB, which is essentially an artefact of the model.

One difficulty in constructing compensated models is

^{*} Email: anthony@mrao.cam.ac.uk

that the initial density and velocity profiles must be chosen in such a way that streamline crossing is avoided. Without this, shock fronts form and one would have to include pressure to produce a realistic model. For example, if one just perturbs the density profile without perturbing the velocity field, then streamline crossing is inevitable in any compensated model other than those of ‘Swiss cheese’ type (where the problem would only occur in the vacuum region).

Here we discuss a family of models which avoid the problem of streamline crossing in a very simple manner, while keeping the density profile compensated and realistic. The initial perturbation is of finite extent and is controlled by two physical parameters, one describing the magnitude of the perturbation and the other its linear extent. The perturbation drops to zero at a finite radius, beyond which the Universe is described by an FRW model. A third parameter, m , controls the degree of the polynomial describing the perturbation and can be adjusted to produce the desired structure in the nonlinear regime. The two parameters controlling the perturbation and the further two parameters describing the external universe uniquely determine the form of the velocity perturbation for each polynomial degree. This is achieved by matching the first m derivatives at the centre and edge of the perturbation, leaving a polynomial of degree $2m + 1$. From the velocity profile the density perturbation is uniquely fixed by the constraints that there are no decaying modes present and that the density distribution is compensated. In these models density compensation holds at all later times and the velocity field evolves in a way that avoids streamline crossing. The fact that the initial density and velocity profiles are described by simple polynomials also simplifies the task of carrying out accurate numerical work.

In this paper we describe the theoretical aspects of our model and provide a detailed comparison with other work. In Section 2 we introduce a novel way of treating the field equations for spherically symmetric dust, which arose from a new, gauge-theoretic treatment of gravity presented elsewhere (Lasenby, Doran & Gull 1998). This method works with a single global time coordinate which reduces the equations to an essentially Newtonian form. The insights provided by this gauge lead naturally to the idea of specifying initial conditions on a surface of constant ‘Newtonian’ time, and we show how to parameterise the matter streamlines to take advantage of this possibility.

In Section 3 the equations for photon propagation are presented, and we derive a simple formula for the temperature decrement induced in the CMB by the cluster. We also derive a new formula for density evolution along a streamline. This considerably simplifies the task of computing the density profile at later times. The advantages of our gauge choices are further illustrated by linearising the field equations to produce a relation between the velocity and density profiles for realistic initial conditions. In Section 4 we discuss Swiss Cheese models and give a new formula for the CMB temperature decrement in such models. We also consider the strengths and limitations of these models as a prelude to presenting an improved scheme.

Our improved model is presented in Section 5. Despite the simplicity of the model, numerical simulations reveal that the initial perturbation evolves to produce a density profile which accurately matches the King profile ob-

served in many galaxy clusters. The main limitations of our model concern the imposition of spherical symmetry and the lack of pressure support in the evolving cluster. Both assumptions lead to large cluster infall velocities relative to the CMB, and these are certainly much larger than the velocities observed in nearby clusters. However, recent numerical work (Navarro, Frenk & White 1996) has suggested that large infall velocities might occur in evolving clusters at higher redshifts, for which our model would then be well suited. For example, the microwave decrements associated with quasar pairs reported by Jones et al. (1997) and Richards et al. (1997) may be due to combined Sunyaev-Zel’dovich and gravitational effects from high redshift clusters. This is discussed further in an accompanying paper (Dabrowski et al. 1997), where the theoretical model for the gravitational effect described here is implemented numerically. Some results of this analysis are briefly discussed in the concluding section. Natural units $G = c = \hbar = 1$ are employed throughout.

2 THE FIELD EQUATIONS AND THE NEWTONIAN GAUGE

The equations used here were first derived by Lasenby, Doran & Gull (1995) using a new, gauge-theoretic approach to gravity. This approach employed ‘geometric algebra’, the mathematical language which seems to capture best the nature of the gauge fields and the structure of the equations. Despite the different conceptual foundations of the theory developed by Lasenby et al. (1998), the predictions of the theory agree with general relativity for a wide range of phenomena, and for the systems studied here the two theories agree exactly. So as not to alienate readers unfamiliar with geometric algebra, we have not employed it in this paper, and have instead adopted an approach closer to that of standard general relativity. The price of this approach is that some of the results employed below are quoted without proof from Lasenby et al. (1998).

The system we study in this paper consists of a spherically symmetric distribution of dust. Modifications to include either pressure or a cosmological constant are not considered here. Lasenby et al. (1998) showed that a natural gauge emerges for the analysis of such systems. This gauge is global, employing a single time coordinate t and a radial coordinate r . The time coordinate t measures the free-fall time for observers comoving with the fluid. In inhomogeneous regions the radial coordinate r is related to the strength of the tidal force defined by the Riemann tensor. The key dynamical variables are the density $\rho(t, r)$, a velocity field $u(t, r)$ and a generalised ‘boost’ factor denoted by $\Gamma(t, r)$. (In Lasenby et al. (1998) and (1995), Γ was denoted by g_1 and u was denoted by g_2 .) The fields Γ and u define the line element by

$$ds^2 = \left(1 - \frac{u^2}{\Gamma^2}\right) dt^2 + 2\frac{u}{\Gamma^2} dt dr - \frac{1}{\Gamma^2} dr^2 - r^2(d\theta^2 + \sin^2\theta d\phi^2), \quad (1)$$

where θ and ϕ are standard polar coordinates, $0 \leq \theta \leq \pi$, $0 \leq \phi < 2\pi$. The density $\rho(t, r)$ defines a total gravitational mass $M(t, r)$ by

$$M(t, r) \equiv \int_0^r 4\pi s^2 \rho(t, s) ds, \quad (2)$$

and the variables Γ , u and M are related by

$$\Gamma^2 = 1 - 2M/r + u^2. \quad (3)$$

If we rewrite this equation in the form

$$\frac{1}{2}u^2 - M/r = \frac{1}{2}(\Gamma^2 - 1) \quad (4)$$

we see that it has a simple, Newtonian interpretation: it is a Bernoulli equation for zero pressure and non-relativistic energy $(\Gamma^2 - 1)/2$.

The variable u defines the integral curves of the conserved fluid current by

$$\frac{dr}{dt} = u. \quad (5)$$

These integral curves are also matter geodesics, since there is no pressure present. The key dynamical equations are update equations along these fluid streamlines, for which we require the comoving derivative

$$\frac{D}{Dt} \equiv \frac{\partial}{\partial t} + u \frac{\partial}{\partial r}. \quad (6)$$

The total gravitational mass enclosed, M , is conserved along the fluid streamlines,

$$\frac{DM}{Dt} = 0. \quad (7)$$

Implicit here is the assumption that the initial conditions are chosen to avoid the possibility of streamline crossing. The Euler equation in this setup is

$$\frac{Du}{Dt} = -\frac{M}{r^2}. \quad (8)$$

It follows that

$$\frac{D\Gamma}{Dt} = 0. \quad (9)$$

The above set of equations look Newtonian, yet they are fully consistent with general relativity. This is the advantage of the gauge choices made to manipulate the equations into the above form. The form of the equations led us to name this gauge the ‘Newtonian’ gauge. Initial data for the above set of equations can be given in a variety of forms, but the most natural is to specify the density $\rho(t_i, r)$ and the velocity $u(t_i, r)$ at some initial time t_i . From these one can calculate $M(t_i, r)$ and $\Gamma(t_i, r)$, which are then conserved along the streamlines.

To complete the set of basic equations it is useful to introduce the velocity gradient H :

$$H(t, r) \equiv \frac{\partial}{\partial r} u(t, r). \quad (10)$$

From the above equations it is straightforward to show that

$$\frac{D\rho}{Dt} = -(2u/r + H)\rho. \quad (11)$$

The function H is shown below to play a fundamental role in determining the temperature fluctuations caused by an infalling cluster.

The above set of equations have analytic solutions which were first found by Tolman (1934) and Bondi (1947). The difference between the above approach and the Tolman solution is that Tolman used M as the radial coordinate, instead

of r . This has the disadvantage of hiding the Newtonian nature of the equations, making it hard to visualise the physics. The form of the analytic solution to the above equations depends on the sign of $\Gamma^2 - 1$ on the initial timeslice. There are three cases to consider:

1. $\Gamma^2 < 1$

For this case the matter streamlines (geodesics) are defined by

$$r = \frac{M}{1 - \Gamma^2} (1 - \cos\eta) \quad (12)$$

$$t - t_i = \frac{M}{(1 - \Gamma^2)^{3/2}} (\eta - \sin\eta - \eta_i + \sin\eta_i) \quad (13)$$

where η parameterises the curve and η_i is determined from the initial value of r at time t_i . The quantities M and Γ are constant along the curve. In order to choose the initial value of η correctly, one needs the further result that

$$u = \frac{M}{r(1 - \Gamma^2)^{1/2}} \sin\eta \quad (14)$$

so that η_i is uniquely fixed between $0 < \eta_i < 2\pi$ from a knowledge of whether the initial velocity is inwards or outwards. The case $\eta_i = \pi$ corresponds to starting from rest, as treated by Lasenby et al. (1998).

2. $\Gamma^2 = 1$

This case includes a flat FRW cosmology, and the equations can be integrated directly to give

$$t - t_i = \frac{2}{3} \frac{(r^{3/2} - r_i^{3/2})}{(2M)^{1/2}}. \quad (15)$$

The velocity is chosen to be outwards to avoid a singularity forming instantaneously.

3. $\Gamma^2 > 1$

This case includes open cosmologies. The matter curves are parameterised as follows:

$$r = \frac{M}{\Gamma^2 - 1} (\cosh\eta - 1) \quad (16)$$

$$t - t_i = \frac{M}{(\Gamma^2 - 1)^{3/2}} (\sinh\eta - \eta - \sinh\eta_i + \eta_i) \quad (17)$$

and the velocity is given by

$$u = \frac{M}{r(\Gamma^2 - 1)^{1/2}} \sinh\eta. \quad (18)$$

For this case it is also necessary to start with an initial outward velocity to avoid streamline crossing.

The above parameterised expressions for the matter streamlines are more general than those usually presented (Panek 1992). This is necessary so that the initial data can be specified on a constant t timeslice, which provides better control over the form of the initial perturbations. The initial time t_i is arbitrary and is usually either set to zero or chosen so that the present epoch corresponds to $t = 0$. Initial data is defined by $\rho(t_i, r)$ and $u(t_i, r)$ and from these the initial values of M and Γ are found. At the initial point $r(t_i)$ the value of η_i is found, and the resulting

curves are plotted parametrically. Examples of these curves for collapsing dust are given by Lasenby et al. (1998). The lack of pressure support means that infalling matter collapses to a singularity in a finite time. This does not pose any problems, provided photons passing through the cluster do not encounter a singularity or horizon.

3 PHYSICS IN THE NEWTONIAN GAUGE

There seems little doubt that the Newtonian gauge provides the cleanest description of gravitational physics for spherically symmetric systems (Lasenby et al. 1998; Lasenby et al. 1997a) and it is surprising that it is not more widely used. Here we review here some key physical results from the Newtonian gauge perspective. These results are employed in later sections to construct numerical models. A further illustration of the use of the Newtonian gauge which is slightly outside the main theme of this paper is contained in Appendix A.

3.1 Cosmology

While the Newtonian gauge arises naturally in the study of spherically symmetric systems, it is not immediately apparent that it is valuable in the study of homogeneous cosmological models. Since the models we discuss below contain a homogeneous region outside the perturbed region, it is useful to see how standard cosmological notions fit into this scheme (see also Gautreau (1984) and Ellis & Rothman (1993) for similar, more detailed discussions).

In a homogeneous model the density ρ is a function of time t only, so we have

$$M(r, t) = \frac{4}{3}\pi r^3 \rho(t). \quad (19)$$

Equations (7) and (11) now yield $H = u/r$ and $\dot{\rho} = -3H\rho$, where the overdot denotes differentiation with respect to time. It follows that H is a function of time only for homogeneous models.

The Euler equation (8) yields the second cosmological equation,

$$\dot{H} + H^2 = -\frac{4\pi}{3}\rho. \quad (20)$$

It is clear now that we can identify H as the Hubble function and that the Newtonian time parameter agrees with cosmic time in homogeneous regions of the model.

To complete the set of cosmological equations we note from equation (3) that Γ^2 must be of the form

$$\Gamma^2 = 1 + r^2\chi(t). \quad (21)$$

Conservation of Γ down the streamlines (equation (9)) shows that

$$\dot{\chi} = -2H(t)\chi, \quad (22)$$

hence we have

$$\Gamma^2 = 1 - kr^2 \exp\left\{-2 \int^t H(t') dt'\right\}. \quad (23)$$

The Friedmann equations in their standard form (with zero pressure and cosmological constant) are recovered by introducing the scale factor $S(t)$ via the definition

$$H(t) = \frac{\dot{S}(t)}{S(t)}, \quad (24)$$

so that

$$\Gamma^2 = 1 - kr^2/S^2, \quad (25)$$

with $k = 0, \pm 1$ determining the type of cosmology in the usual manner.

In the Newtonian gauge version of cosmology, particles in the Hubble flow are pictured as moving radially outwards at a velocity $\dot{r} = H(t)r$. The expansion centre is not a physical feature, since the model is homogeneous and all gauge-invariant (measurable) quantities are functions of time only. One can often take advantage of this fact by considering observers located at the origin. This provides a novel way of visualising some of the less intuitive aspects of FRW cosmologies (Lasenby et al. 1998). Along the matter streamlines $r(t)/S(t)$ is constant. The standard ‘co-moving’ gauge for cosmology is obtained by introducing a new radial coordinate $R = r/S$, so that the matter geodesics are lines of constant R .

3.2 Photon Paths and Redshifts

In studying photon trajectories it is sufficient to just consider motion in the $\theta = \pi/2$ plane. We can parameterise the photon paths in terms of the Newtonian time parameter t (cosmic time for homogeneous models), so that the path is defined by $r(t)$ and $\phi(t)$. The condition that the trajectory is null means that we can write

$$\frac{dr}{dt} = \Gamma \cos\chi + u \quad (26)$$

$$\frac{d\phi}{dt} = \frac{\sin\chi}{r} \quad (27)$$

where χ is the angle between the photon trajectory and the cluster centre, as measured by observers comoving with the fluid. The geodesic equation is equivalent to the following first-order equation for χ :

$$\frac{d\chi}{dt} = \sin\chi(-\Gamma/r + (H - u/r)\cos\chi). \quad (28)$$

The above set of three first-order equations is simpler to implement numerically than the second-order equations obtained from the direct approach. The equations have the further advantage of dealing directly with the measurable quantities t and χ . It is typical of the gauge theory approach that one obtains first-order equations in the gauge invariant observables such as these. Initial data for the trajectory consists of position data r_i and ϕ_i and a direction χ_i . For most calculations, however, the data is given in the form of the observer’s position and an angle on the sky χ , and the equations are then run backwards in time to take the photon back through the cluster. This is the simplest way to perform lensing simulations.

The remaining content of the geodesic equation concerns the frequency ω in the rest frame of the fluid. This satisfies the equation (Lasenby et al. 1998)

$$\frac{d\omega}{dt} = -\omega\left(H \cos^2\chi + \frac{u}{r} \sin^2\chi\right). \quad (29)$$

It is not hard to show that the above equations imply that the angular momentum $L = \omega r^2 \dot{\phi} = -r\omega \sin\chi$ is conserved.

For the case of a homogeneous cosmology, the redshift equation (29) reduces to

$$\frac{d\omega}{dt} = -\omega H, \quad (30)$$

from which we recover the standard result that ωS is constant for a photon travelling in a homogeneous, dust-filled Universe. This result shows how the standard predictions of cosmology are recovered in this unfamiliar gauge.

To calculate the effect of a cluster on the CMB, we write

$$u(t, r) = rH_e(t) + \Delta(t, r), \quad (31)$$

where $H_e(t)$ is the Hubble function in the exterior Universe at the same time t , and Δ is the difference between the equivalent velocity of the unperturbed Universe and the cluster velocity. For a photon passing through the cluster we find that

$$\frac{d}{dt} \ln(\omega S) = -\frac{\partial \Delta}{\partial r} \cos^2 \chi - \frac{\Delta}{r} \sin^2 \chi. \quad (32)$$

We therefore define the function

$$\epsilon = \int_{t_1}^{t_2} dt \left(\frac{\partial \Delta}{\partial r} \cos^2 \chi + \frac{\Delta}{r} \sin^2 \chi \right), \quad (33)$$

where the integral is evaluated along the photon path between the time the photon enters the cluster (t_1) and the time it leaves (t_2). The function ϵ is small, since the contribution to the integral from near the cluster centre tends to cancel the contributions from further out. The main effect producing a non-zero ϵ is essentially the evolution of Δ with time.

If the photon enters the cluster from the CMB with frequency ω_1 and reemerges with frequency ω_2 we have

$$\omega_2' = \omega_1 \frac{S(t_1)}{S(t_2)} e^{-\epsilon}. \quad (34)$$

An equivalent unperturbed photon will have frequency

$$\omega_2 = \omega_1 \frac{S(t_1)}{S(t_2)}, \quad (35)$$

so the physically measurable temperature decrement is

$$\frac{\Delta T}{T} = \frac{\omega_2' - \omega_2}{\omega_2} = e^{-\epsilon} - 1 \approx -\epsilon. \quad (36)$$

This simple result enables easy computation of the effect of the cluster for various angles on the sky.

3.3 Evolution of the Physical Variables

The two key physical variables required at later times are the density distribution, which should evolve to produce a realistic distribution for a cluster, and the velocity gradient, which controls the propagation of photons through the cluster. One way to calculate these at later times is to differentiate numerically the mass $M(t, r)$ and velocity, which are easily found on any given streamline. A better approach, however, is to construct explicit analytical formulae for ρ and H on a given streamline, which we now discuss.

We start with the density profile and employ the relation

$$\rho(t, r) = \left(\frac{\partial r_i}{\partial r} \right)_t \frac{r_i^2}{r^2} \rho(r_i), \quad (37)$$

which gives $\rho(t, r)$ as a function of the initial density profile $\rho(r_i) = \rho(t_i, r_i)$ and the derivative of the streamline starting position $r_i(t, r)$ with respect to r . To calculate this latter term we use the reciprocity relation

$$\left(\frac{\partial r_i}{\partial r} \right)_t \left(\frac{\partial r}{\partial t} \right)_{r_i} \left(\frac{\partial t}{\partial r_i} \right)_r = -1 \quad (38)$$

to deduce that

$$\left(\frac{\partial r_i}{\partial r} \right)_t^{-1} = -u \left(\frac{\partial t}{\partial r_i} \right)_r. \quad (39)$$

The final term can be calculated directly from the parameterised form of the streamlines. It is convenient here to introduce the function

$$f(r_i) \equiv \Gamma(t_i, r_i)^2 - 1. \quad (40)$$

With this we find that, for $f \neq 0$,

$$\begin{aligned} \left(\frac{\partial r_i}{\partial r} \right)_t^{-1} &= -\frac{1}{2f(r_i)M(r_i)} \left[M(r_i) \frac{df(r_i)}{dr_i} (2r - 3ut) \right. \\ &\quad \left. - 8\pi r_i^2 \rho(r_i) f(r_i) (r - ut) \right] \\ &\quad + \frac{uM(r_i)}{f(r_i)u(r_i)} \frac{d}{dr_i} \left(\frac{r_i f(r_i)}{M(r_i)} \right), \end{aligned} \quad (41)$$

where $M(r_i) = M(t_i, r_i)$ is the initial mass function. With this result one need only compute df/dr_i from the initial data to find the value of ρ on a given streamline. The case of $f = 0$ must be treated separately and yields simply

$$\left(\frac{\partial r_i}{\partial r} \right)_t^{-1} = \left(\frac{r_i}{r} \right)^{1/2} + \frac{ut}{2M(r_i)} 4\pi r_i^2 \rho(r_i). \quad (42)$$

The same technique is used to find the velocity gradient on a streamline at later times. On differentiating equation (3) we find that

$$\frac{\partial u}{\partial r} = -\frac{M}{r^2 u} + \left(\frac{\partial r_i}{\partial r} \right)_t \left(\frac{1}{r} \frac{dM(r_i)}{dr_i} + \frac{1}{2} \frac{df(r_i)}{dr_i} \right), \quad (43)$$

which again gives H on a streamline in terms of the streamline label r_i and the initial data. These formulae are very useful for carrying out accurate numerical simulations.

3.4 The Linearised Equations

We now derive a physical constraint on the initial conditions for our model by considering evolution in the linear regime. Linearising the field equations around a homogeneous background cosmology is a straightforward exercise in the Newtonian gauge. We start by introducing the variables

$$\delta u \equiv u - r\bar{H}(t) \quad (44)$$

$$\delta \rho \equiv \rho - \bar{\rho}(t) \quad (45)$$

$$\delta M \equiv \int_0^r 4\pi s^2 \delta \rho(t, s) ds, \quad (46)$$

where the barred quantities denote the background homogeneous values. The linearised equations for the velocity field now yield

$$\frac{D \delta u}{Dt} = -\frac{\delta M}{r^2} - \bar{H} \delta u \quad (47)$$

and

$$\frac{D}{Dt} \left(\frac{D\delta u}{Dt} \right) + 3\bar{H} \frac{D\delta u}{Dt} - \bar{H}^2 \delta u = 0, \quad (48)$$

where we have assumed that the background is described by a spatially flat, $\Lambda = 0$ cosmology. Equation (48) shows that the evolution of the density perturbation down the streamline is determined entirely by the background cosmology, and not by the local properties of the perturbation. It follows that there is nothing special about the assumption of spherical symmetry and equation (48) is a general result for the growth of a velocity perturbation in a dust-filled cosmology.

We can parameterise δu in terms of a streamline starting point and cosmic time t . In this way the streamline derivatives are replaced by derivatives with respect to t , and we arrive at the equation

$$\delta\ddot{u} + 3\bar{H} \delta\dot{u} - \bar{H}^2 \delta u = 0. \quad (49)$$

Since $\bar{H} = 2/(3t)$ we see that δu has modes going as $t^{1/3}$ and $t^{-4/3}$. Only the former of these is growing with respect to the background value. If we assume that we are in an epoch when the decaying mode can be ignored, we find that

$$\frac{D\delta u}{Dt} = \frac{1}{2} \bar{H} \delta u. \quad (50)$$

It follows that the density and velocity perturbations in the linear regime, when no decaying modes are present, are related by

$$\frac{3}{2} \bar{H} \delta u = -\frac{\delta M}{r^2}. \quad (51)$$

This provides a constraint on the initial conditions for our models.

4 SWISS CHEESE MODELS

The most popular method to date for theoretical calculations of CMB anisotropies in the nonlinear regime has been to employ ‘Swiss Cheese’ models (Rees & Sciama 1968; Nottale 1982a). In these models an overdense collapsing region is surrounded by a compensating vacuum region which then matches onto the external Universe. Nottale (1982a) developed a complicated set of equations for describing photon redshifts in such a model. The interior region is modelled by a collapsing $\Omega > 1$ cosmology, and three coordinate systems are employed with two sets of matching equations at the boundaries. Initial data consists of the set $\{H_0, \rho_0, H_c, \rho_c, r_i, z_c\}$, where H_0 and ρ_0 are the values of the Hubble constant and density at the present epoch, H_c and ρ_c are the equivalent variables for the central cluster region as the photon passes through the centre, z_c is the redshift of a photon emitted from the centre of the cluster at the epoch described by H_c and ρ_c , and r_i is the cluster radius when the photon exits the central core. One of the five dimensional quantities is arbitrary and can be scaled to unity, so Nottale’s setup defines a five-parameter model. To analyse this it is convenient to introduce a set of dimensionless variables. Along with z_c these consist of the two deceleration parameters q_c and q_0 , together with

$$y \equiv H_c r_i \quad \text{and} \quad h \equiv \frac{H_c}{H_0}. \quad (52)$$

It is also convenient to define

$$n = \left(\frac{\rho_c}{\rho_0} \right)^{1/3} = \left(\frac{q_c}{q_0} \right)^{1/3} h^{2/3}. \quad (53)$$

From the initial data it is possible to calculate the redshift of a photon as it reemerges into the exterior Universe given its redshift at the centre z_c . The method relies on the fact that the initial data define the epoch when the photon is at the cluster centre. First H_c , ρ_c , r_i and z_c are used to calculate the redshift of the photon at the edge of the collapsing region. This step is a straightforward application of the Mattig relation (Peebles 1993, Chapter 13). Next one computes the photon redshift after it crosses the void region and enters the exterior Universe. This calculation is possible because of the existence of a timelike Killing vector in the vacuum region, which ensures that $\omega(\Gamma + u)$ is constant as the photon crosses the vacuum. From this it is possible to calculate the redshift of the photon as it reenters the unperturbed Universe as a function of the input variables. A similar, more involved calculation is performed in the opposite time direction to obtain the total photon redshift across the perturbed region. This redshift is then compared with that of a photon coming from an unperturbed region of the Universe to obtain a central temperature decrement.

The resultant equations are complicated and cannot be solved analytically. Nottale (1982a) obtained a power series solution by expanding in both y (which is necessarily small) and z_c . A better approach, however, is to obtain an expression valid for general z_c using only an expansion in y . This calculation is tricky, but with the help of the symbolic algebra package Maple it is possible to perform such an expansion. The result, which we give here for the first time, is

$$\begin{aligned} \frac{\Delta T}{T} &= -4q_0 \left(\frac{ny}{h} \right)^3 \left\{ (1+z_c)(1+2q_0 z_c)^{1/2} \right. \\ &\quad \left. \times \left[1 - \ln \left(\frac{n}{1+z_c} \right) \right] - h \right\}. \end{aligned} \quad (54)$$

That one can derive an equation such as (54) is somewhat surprising. From the Newtonian gauge perspective, the initial data appears to under-determine the system. This is illustrated in Figure 1, which shows that the velocity profile is not uniquely specified since various curves can be fitted in the vacuum region. Different curves produce different crossing times for photons to cross the vacuum region and so produce different physical models. The trick which makes the derivation of (54) possible is that z_c is specified as part of the initial data. This effectively places an extra constraint on the form of the velocity function in the vacuum and, while not pinning down the form of the curve uniquely, this does render the predictions unique. The residual freedom in the choice of velocity function amounts to a gauge freedom so has no physical significance.

While the result (54) provides a useful estimate of the effect of a cluster, this type of Swiss Cheese model has a number of weaknesses. The density distribution is highly unrealistic and must limit the accuracy of any predictions from such models. The same can be said of the high infall velocities in such models, which appear to overestimate the CMB temperature decrement. A further weakness is the number of arbitrary parameters in the model. While the cluster width, density and redshift are certainly sensible parameters for such a model, the velocity in the form of H_c

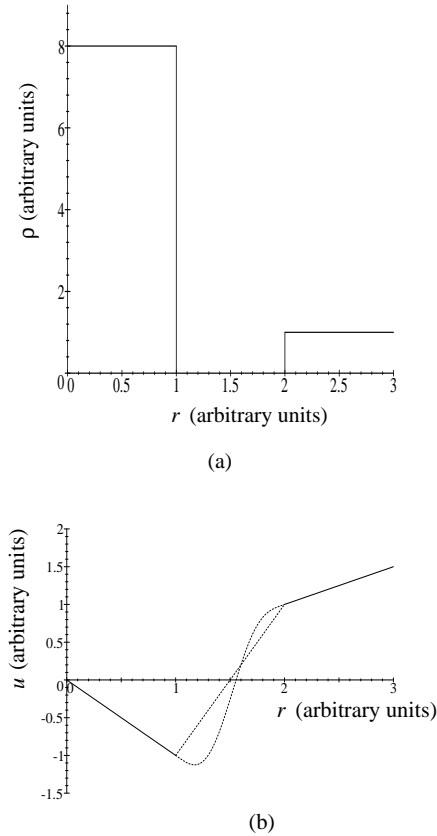


Figure 1. *Initial Data for Swiss Cheese Models.* (a) shows the initial density distribution, with a uniform central overdensity and a compensating vacuum. The width of the compensating region ensures that the total mass enclosed is the same as would have been enclosed if the density was uniformly distributed with the exterior value. (b) shows the initial velocity distribution. The central region is modelled by a collapsing $\Omega > 1$ Universe, and the exterior region by an arbitrary, expanding model. There is no unique curve extrapolating the initial velocity distribution across the vacuum. Two different curves are shown, which would produce two different models.

or h is not an obvious physical parameter. Nottale addressed this weakness in a later paper (Nottale 1984) by introducing the additional restriction that the two matter regions issued from the same singularity. This correlates the (Newtonian) times in the internal and external regions, and allows one to determine h in terms of the remaining dimensionless parameters. This assumption is partially supported by Silk’s result that the effect of eliminating the decaying modes is to set the time that each streamline leaves the initial singularity to a constant value (Silk 1977). This result only holds in the linear theory, however, so it is not obviously applicable to Swiss Cheese models. In the following section we propose an alternative model which addresses these weaknesses in a simple and elegant manner.

5 SIMPLE, FOUR-PARAMETER MODELS

The control over the initial conditions afforded by the Newtonian gauge approach provides for many models of the development of a perturbation away from a homogeneous cosmology. Here we discuss a family of simple four-parameter models based on polynomial perturbations in the density and velocity fields. The perturbation is of finite extent and the density distribution is compensated. The region outside the perturbation therefore evolves as a homogeneous cosmology, and placing observers in this region allows for unambiguous calculations of the CMB perturbation caused by the cluster. The perturbation is assumed to have grown from primordial fluctuations in the very early universe, and to still be well described by the linearised Einstein equations. We therefore expect that the decaying modes are negligible at the epoch when we specify the initial conditions. This physical requirement is imposed by ensuring that the initial velocity and density profiles satisfy equation (51).

In our model the velocity perturbation is controlled by two physical parameters — one specifying the width of the perturbation, and the other the velocity gradient at the origin. For models of cluster formation the velocity gradient at the origin is slightly less than that of the unperturbed Universe. Voids can be modelled with a slightly greater velocity gradient. A third parameter m controls the degree of the polynomial describing the perturbation, and is chosen to ensure a realistic density profile in the nonlinear region. The polynomial describing the velocity perturbation has degree $2m + 1$ and is formed as follows. At the centre we have $u = 0$ and the velocity gradient is given. All other derivatives up to order m are set to zero. At the edge we match u and its first m derivatives to the exterior value, $u = rH_i$. These boundary conditions specify a unique curve for each value of m . Curves with $m=2$ and 4 are shown in Figure 2.

With the velocity profile determined, the density profile is found from equation (51). The initial data for the exterior universe consists of a value for the Hubble function H_i and the density ρ_i . With the perturbation width given by r_i , we can introduce the dimensionless variables

$$x = \frac{r}{r_i}, \quad v(x) = \frac{u(r, t_i) - rH_i}{r_i H_i}, \quad f(x) = \frac{\rho(r, t_i) - \rho_i}{\rho_i}. \quad (55)$$

In terms of these, equation (51) takes the form

$$x^2 f(x) = -\frac{d}{dx}(x^2 v(x)). \quad (56)$$

Since $v(x)$ is a degree $2m + 1$ polynomial, $f(x)$ is a polynomial of degree $2m$. Computing the density distribution in this manner ensures that it is compensated at the boundary. The external values of ρ_i and H_i , together with the magnitude and width of the perturbation, form a set of four parameters, one of which is arbitrary because of the freedom to rescale. The initial density and velocity perturbations are given by polynomials, so the function $f(r_i) = \Gamma(r_i)^2 - 1$ also has a simple polynomial expression. It follows that all of the terms on the right-hand side of equation (41) can be calculated algebraically, enabling accurate computation of the density on a given streamline.

An example of the streamlines resulting from such an initial setup is shown in Figure 3. The perturbed region has a slight undervelocity, so after a finite time it starts to recollapse and form a compact cluster. The figure illustrates

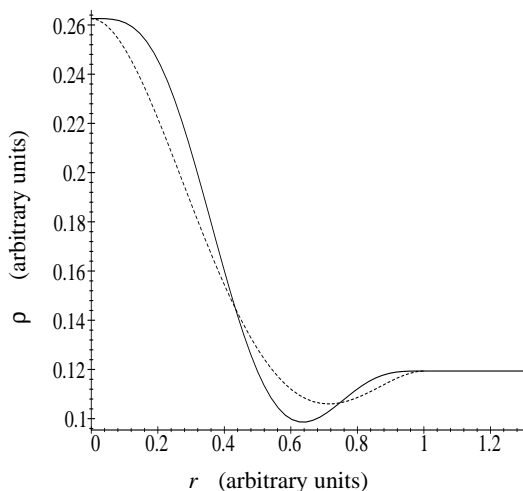
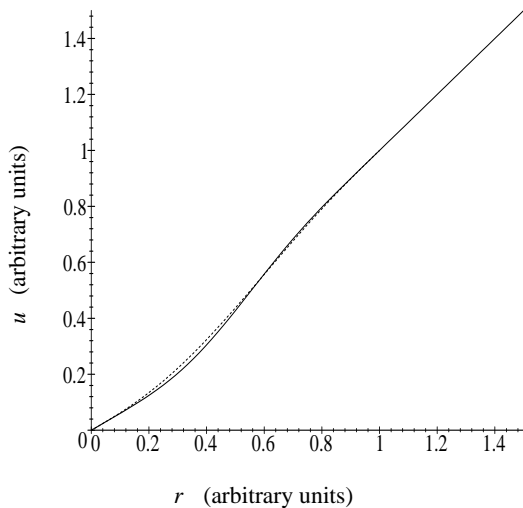


Figure 2. *Initial data for the 4-parameter model.* The solid curves are for $m = 4$ and the dashed curves for $m = 2$. The perturbation has radius $r_i = 1$ (arbitrary units), beyond which the velocity $u(t_i, r)$ is proportional to r and the density is uniform. The perturbation is defined by the velocity gradient at the origin (set to 0.6 here) and the radius r_i . The density profile is compensated, so the total mass enclosed in $r < r_i$ is the same as would have been enclosed if the initial density was uniform.

that streamline crossing does not occur in our models. An example of the density distribution resulting from growing this perturbation is shown in Figure 4. This density distribution closely matches the King profile observed in galaxy clusters (Dabrowski et al. 1997), a remarkable result given the simplicity of the model.

The fact that the density distribution evolves to a realistic profile makes it possible to choose input parameters to achieve realistic simulations of the effect of a cluster. A photon can then be sent through the cluster to simulate the

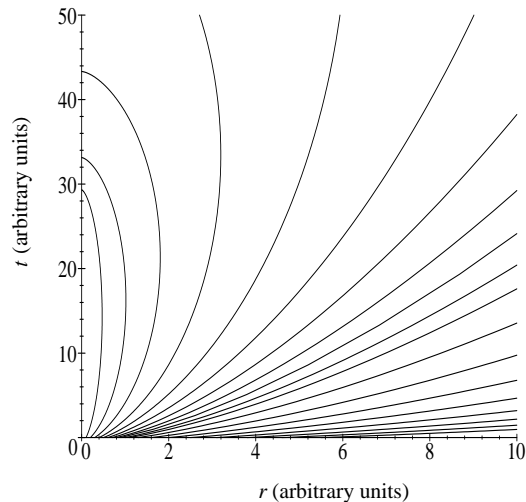


Figure 3. *Matter streamlines for an $m = 3$ model.* The perturbation has initial width 1, with $H_i = 1$ and $\rho_i = 3/(8\pi)$. The velocity gradient at the centre of the perturbation is 0.95. The central region is moving inwards relative to the Hubble flow, so recollapses to a singularity in a finite time. The form of the initial data ensures that streamline crossing does not occur.

effect on the CMB. The epoch at which the photon enters the cluster region is the fourth physical parameter in the model. One can then perform detailed calculations of the lensing properties of the cluster and its effect on the CMB. These are contained in an accompanying paper (Dabrowski et al. 1997).

The main limitation with the model presented here is the lack of pressure support. This has two effects. First, the infall velocities in the cluster are unrealistically large compared to a virialised cluster. This will tend to overestimate the temperature decrement due to the cluster, since it is the evolution of the velocity difference $\Delta(t, r)$ with time which is central in determining the magnitude of the perturbation. The second effect is that a central singularity forms too soon, when the first streamline reaches the origin. There are no difficulties in extending the model beyond this time, provided the photon has exited the cluster before the horizon has formed, but the initial conditions must ensure that singularities do not form at early epochs. It turns out that introducing the perturbation at recombination does not pose any problems numerically, and we typically set our initial conditions at $z = 1000$.

6 CONCLUSIONS

We have shown that both spherically symmetric collapse and cosmology can be studied in a single global coordinate system, which we have called the Newtonian gauge. This gauge considerably simplifies the task of modelling cluster formation and its effects on the CMB. Observers can be placed in a region of the model corresponding to an FRW Universe, and

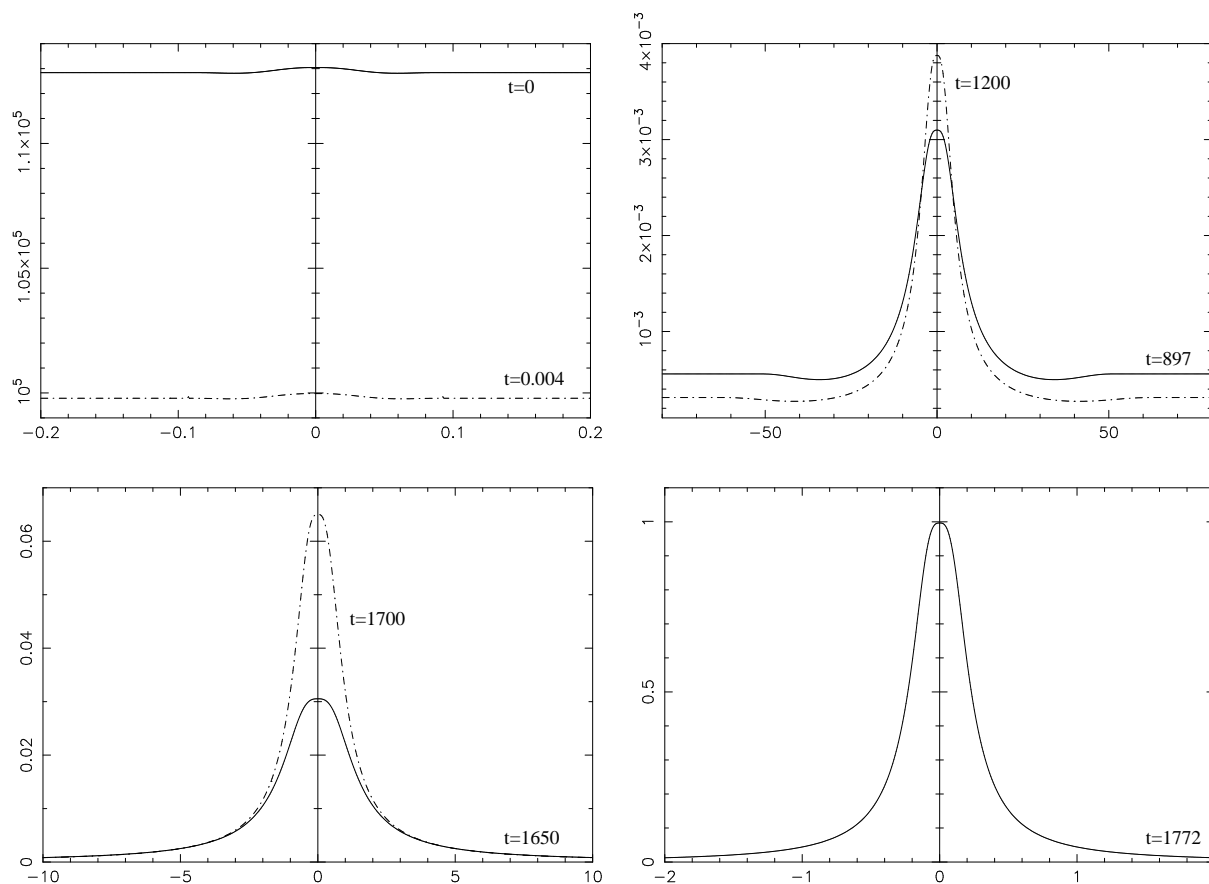


Figure 4. Density evolution for an $m = 3$ model. The initial density profile contains a small, compensated perturbation around the background level. Initially, the density falls with the expansion of the Universe. After $t = 897$ the streamlines turn round, the central region starts to collapse and the density there increases. The perturbation evolves to give the final density distribution shown at $t = 1772$. This closely matches the observed density profiles in galaxy clusters (Dabrowski et al. 1997). The units are arbitrary.

both the lensing and CMB temperature decrement are easily modelled. In an accompanying paper (Dabrowski et al. 1997) detailed computations are performed with this model and compared with other work and with observations. Numerical integration along photon paths are performed to compute the lensing effects of the cluster. The effects on the CMB power spectrum are also computed by evolving a simulated background (with Gaussian fluctuations) through the cluster to the observer.

A study of Swiss Cheese models within the Newtonian gauge revealed the surprising result that the models only yield unique predictions because of the particular way the initial data is given. A new formula for the CMB temperature decrement in a Swiss Cheese model was presented, and it was argued that the number of arbitrary parameters in such models limits their usefulness.

The problems with Swiss Cheese models are overcome in a simplified model in which a small density and velocity perturbation is introduced at recombination and allowed to grow to give a compensated density profile. The centre of this density distribution models a cluster with a density profile close to that of the King profile. Photons can then be sent through this density distribution to model the effects of clusters at arbitrary redshifts. The lack of pressure

support means that the model probably over-estimates the perturbations induced in the CMB. This will certainly be the case for nearby clusters which are virialised and do not have large infall velocities. Recent work on structure formation, however, has suggested that clusters with large infall velocities could well have formed around redshifts of 2 and higher. If so, the model presented in this paper could prove very useful for calculating the effects of such clusters.

ACKNOWLEDGEMENTS

We thank an anonymous referee for useful comments. CD thanks the Lloyd's of London Tercentenary Foundation for their financial support. MPH thanks Trinity Hall, Cambridge, for their support in the form of a research fellowship.

REFERENCES

- Arnau J., Fullana M., Monreal L., Sáez D., 1993, *ApJ*, 402, 359
- Arnau J., Fullana M., Sáez D., 1994, *MNRAS*, 268, L17
- Bondi H., 1947, *MNRAS*, 107, 410
- Chodorowski M., 1991, *MNRAS*, 251, 248

- Dabrowski Y., Hobson M., Lasenby A., Doran C., 1997, Microwave background anisotropies and nonlinear structures II. Numerical Computations, submitted to MNRAS
- Dyer C., 1976, MNRAS, 175, 429
- Ellis G., Rothman T., 1993, Am. J. Phys., 61(10), 883
- Fullana M.J., Sáez D., Arnau J.V., 1994, ApJS, 94, 1
- Gautreau R., 1984, Phys. Rev. D, 29(2), 186
- Jones M.E. et al., 1997, ApJ, 479, L1
- Kaiser N., 1982, MNRAS, 198, 1033
- Landau L., Lifshitz E., 1975, The Classical Theory of Fields. (Fourth Edition). Pergamon Press
- Lasenby A., Doran C., Dabrowski Y., Challinor A., 1997a, in Sánchez N., Zichichi A., eds, Current Topics in Astrofundamental Physics, Erice 1996. World Scientific, Singapore, p. 380
- Lasenby A., Doran C., Gull S., 1995, in Sánchez N., Zichichi A., eds, Advances in Astrofundamental Physics, Erice 1994. World Scientific, Singapore, p. 359
- Lasenby A., Doran C., Gull S., 1998, Phil. Trans. R. Soc. Lond. A, 356, 487
- Martínez-González E., Sanz J., 1990, MNRAS, 247, 473
- Martínez-González E., Sanz J., Silk J., 1990, ApJ, 355, L5
- Navarro J., Frenk C., White S., 1996, ApJ, 462, 563
- Nottale L., 1982a, A&A, 110, 9
- Nottale L., 1982b, A&A, 114, 261
- Nottale L., 1983, A&A, 118, 85
- Nottale L., 1984, MNRAS, 206, 713
- Panek M., 1992, ApJ, 388, 225
- Peebles P., 1993, Principles of Physical Cosmology. Princeton University Press, New Jersey
- Pyne T., Birkinshaw M., 1996, ApJ, 458, 46
- Quilis V., Ibáñez J., Sáez D., 1995, MNRAS, 277, 445
- Quilis V., Sáez D., 1998, MNRAS, 293, 306
- Rees M., Sciama D., 1968, Nat, 217, 511
- Richards E.A., Formalont E.B., Kellerman K.I., Partridge R.B., Windhorst R.A., 1997, AJ, 113, 1475
- Sáez D., Arnau J., Fullana M., 1993, MNRAS, 263, 681
- Silk J., 1977, A&A, 59, 53
- Tolman R., 1934, Proc. Nat. Acad. Sci. U.S., 20, 169

$$\Gamma \frac{\partial}{\partial r} \left(\frac{M}{r^3} \right) = \left(\frac{4}{3} \pi \rho - \frac{M}{r^3} \right) 3 \frac{\Gamma}{r}. \quad (\text{A3})$$

From this we can extract Γ/r , and from all of the above measurements we can reconstruct Γ , r and u .

In the homogeneous region, however, this final step is not possible because the right-hand side of (A3) vanishes. This prevents one from determining r from local measurements alone, which is reassuring because in the homogeneous region all local observables should be functions of time only.

APPENDIX A: LOCAL OBSERVABLES

It is instructive to see how one might measure Γ , r and u in the collapsing region with only local measurements of the gravitational field, and to see how the method fails outside the cluster. The key variable is the strength of the radial tidal force. For two objects a (small) proper distance d apart the relative acceleration of one from the other is

$$a = d \left(4\pi\rho - \frac{2M}{r^3} \right). \quad (\text{A1})$$

By measuring the force necessary to prevent this tidal acceleration and comparing this with the local density it is possible to calculate the local value of M/r^3 . Of course, in a homogeneous region this would be just $4\pi\rho/3$.

Next we measure the variation of M/r^3 with time for freely-falling observers. This goes as

$$\frac{D}{Dt} \left(\frac{M}{r^3} \right) = -\frac{3M}{r^3} \frac{u}{r}, \quad (\text{A2})$$

so measurements of this lead to a determination of u/r . It follows from the definition of Γ (3) that the value of $(\Gamma^2 - 1)/r^2$ can also now be determined. Finally, we need to measure the local variation of M/r^3 with proper distance on a constant timeslice. This goes as